

Hyperfine-structure intervals and isotope shifts in the $2p^33s\ ^5S_2 \rightarrow 2p^33p\ ^5P_{J'}$ transitions of atomic oxygen

R. M. Jennerich* and D. A. Tate†

Department of Physics and Astronomy, Colby College, Waterville, Maine 04901

(Received 24 January 2000; revised manuscript received 2 June 2000; published 13 September 2000)

We have measured hyperfine-structure splittings and isotope shifts in the $2p^33s\ ^5S_2 \rightarrow 2p^33p\ ^5P_{1,2,3}$ transitions of atomic oxygen using Doppler-free saturated absorption spectroscopy near 778 nm. Values for the hyperfine-structure coupling constants of the 5S_2 and $^5P_{1,2,3}$ states in ^{17}O and the $^{18}\text{O}-^{17}\text{O}$ and $^{18}\text{O}-^{16}\text{O}$ isotope shifts of the $2p^33s\ ^5S_2 \rightarrow 2p^33p\ ^5P_{1,2,3}$ transitions were found. The set of values for hyperfine-structure coupling constants and isotope shifts is more complete and generally more precise than previously reported results.

PACS number(s): 32.10.Fn, 32.30.Jc

High-resolution spectroscopic measurements on atoms with few electrons are important since experimental data are obtained that can be directly compared with theoretical calculations. Atomic oxygen is the lightest atom with three stable isotopes, and its spectrum has been studied extensively. Of these isotopes, two (^{16}O and ^{18}O) have nuclear spin $I=0$. However, ^{17}O has $I=5/2$, and therefore exhibits hyperfine structure (HFS). In particular, the $2p^33s\ ^5S_2 \rightarrow 2p^33p\ ^5P_{J'}$ (778 nm) and $2p^33s\ ^3S_1 \rightarrow 2p^33p\ ^3P_{J'}$ (845 nm) multiplets of oxygen have been the subject of a number of recent experiments that used Doppler-free spectroscopic techniques [1–4]. Two studies of the $3s\ ^5S_2 \rightarrow 3p\ ^5P_{J'}$ transitions, Marin *et al.* (1992) [3] and Marin *et al.* (1993) [4], have reported values for magnetic dipole (A) and electric quadrupole (B) HF coupling constants for the 5S_2 and 5P_1 states and the isotope shifts (IS) of the $^5S_2 \rightarrow ^5P_1$ transition at a vacuum wavelength of 777.753 nm. These results have stimulated the interest of theorists. Specifically, the magnetic dipole hyperfine-structure constant of the 5S_2 state was calculated using the multiconfiguration Hartree-Fock (MCHF) method [5]. This theoretical analysis included over 71 000 configuration state functions, and yielded a result of $A(^5S_2) = -96.70$ MHz, against an experimental result of -98.59 ± 0.43 MHz [4]. A major difficulty for these calculations was the fact that core polarization due to the $2p$ electrons is a significant effect. The electrons in the closed $1s$ and $2s$ subshells are spin polarized by the exchange interaction with the partially filled $2p$ shell, causing the $2p$ wave function to be nonzero near the nucleus. Were this effect not present, i.e., if the three $2p$ electrons are purely LS -coupled in 4S , and not mixed with other subshells, the $2p^33s\ ^3S$ and $2p^33s\ ^5S$ HFS A constants are expected to be equal in magnitude, but of opposite sign. A comparison of the experimental value for the magnetic dipole HF coupling constant of the $3s\ ^5S_2$ state in ^{17}O with the measured value of A for the $2p^33s\ ^3S_1$ state [4] shows that this prediction is incorrect, and points to a significant contact term in $A(^5S_2)$ that is due to the $2p$ electrons.

The resolution of the previous studies of the $^5S_2 \rightarrow ^5P_{J'}$ multiplet was limited by the observed full width at half-maximum (FWHM) linewidths of approximately 60 MHz in the published spectra, and this precluded measurement of the 5P_2 and 5P_3 HFS intervals from the $^5S_2 \rightarrow ^5P_2$ (777.630 nm) and $^5S_2 \rightarrow ^5P_3$ (777.408 nm) transitions, and the transition IS. In contrast, the natural width of these transitions, predicted from the measured lifetimes of the 5S_2 and $^5P_{J'}$ states, is approximately 4 MHz [6,7]. Motivated by the potential for improved resolution in these transitions, we have made a new investigation of the $^5S_2 \rightarrow ^5P_{J'}$ multiplet, and have obtained spectra with significantly narrower linewidths than those of Refs. [3] and [4]. From our spectra, we obtained values for the hyperfine-structure coupling constants of the 5S_2 and $^5P_{1,2,3}$ states in ^{17}O and the $^{18}\text{O}-^{17}\text{O}$ and $^{18}\text{O}-^{16}\text{O}$ IS of the $2p^33s\ ^5S_2 \rightarrow 2p^33p\ ^5P_{1,2,3}$ transitions. Our results are in good general agreement with the previous data, but generally more precise and extensive.

The experimental apparatus used in this paper is essentially the same as that used in previous studies of atomic fluorine and chlorine [8,9]. A homemade external-cavity diode laser produced a few milliwatts of light at 778 nm [10]. The laser had a spectral linewidth of order 1 MHz, and was tunable over a range of ~ 3 GHz. The Doppler-free absorption signal due to the oxygen atoms was observed using standard saturated absorption techniques. The frequency scale of the laser scan was calibrated using a temperature stabilized 150.127 ± 0.022 MHz free spectral range confocal etalon. Oxygen atoms were generated in the $3s\ ^5S_2$ state from molecular oxygen in a low pressure (less than 0.4 Torr) microwave discharge [11]. The pump and probe-laser beams passed longitudinally through the 6-in.-long discharge region, crossing near the center. The discharge was sustained in a gas mix of at least 80% oxygen, the rest being helium. To obtain spectra of all three stable oxygen isotopes, an isotopically enhanced sample of gas was used (approximately 50% ^{16}O , 40% ^{17}O , and 10% ^{18}O). The spectra were acquired using a digitizing oscilloscope and transferred to a computer. For each of the three members of this multiplet, between 44 and 62 spectra were obtained. The raw data were then analyzed using a commercial software package.

Analysis of the spectra was relatively straightforward. The frequency scale of a spectrum was linearized using the

*Present address: Department of Physics, University of Michigan, Ann Arbor, MI 48109-1120.

†Email address: datate@colby.edu

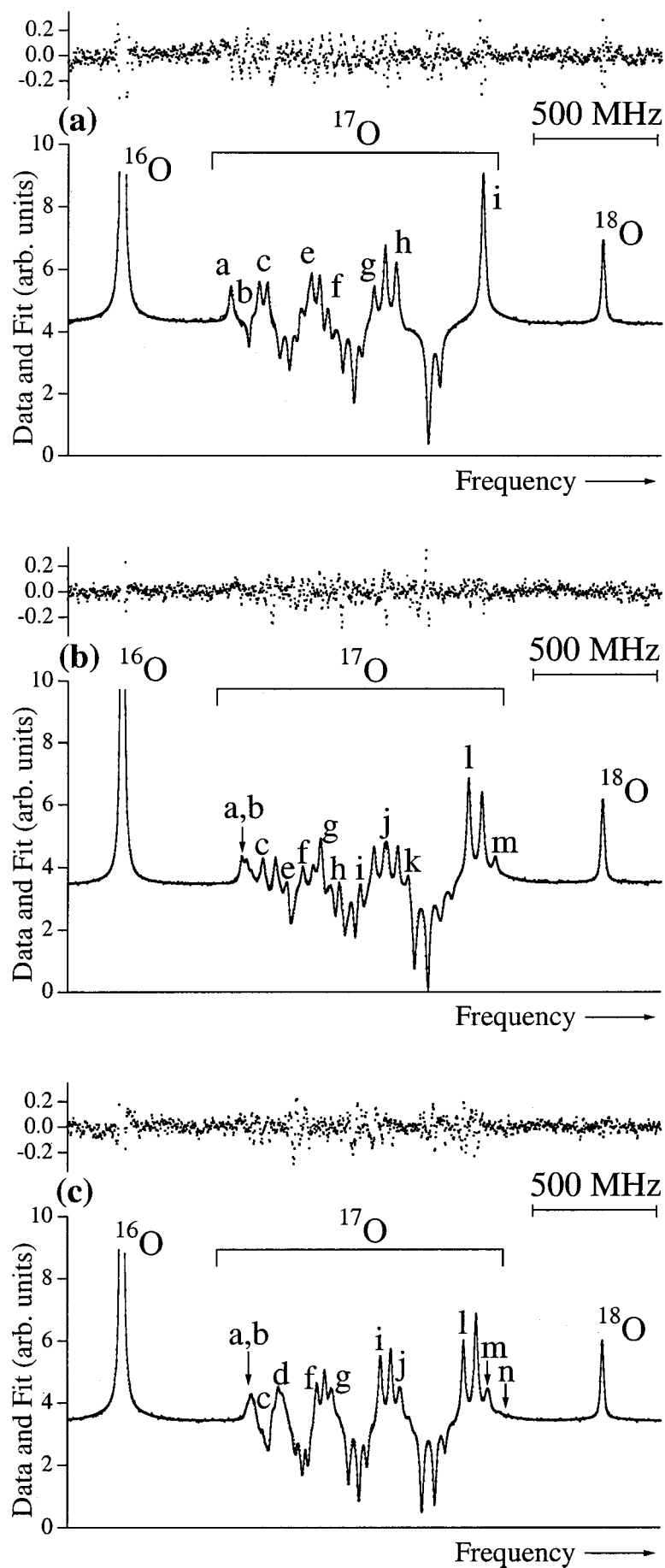


FIG. 1. Doppler-free spectra of the ${}^5S_2 \rightarrow {}^5P_J$ multiplet in atomic oxygen: ${}^5S_2 \rightarrow {}^5P_1$ at $\lambda_{\text{vacuum}} = 777.753$ nm (a); ${}^5S_2 \rightarrow {}^5P_2$ at 777.630 nm (b); and ${}^5S_2 \rightarrow {}^5P_3$ at 777.408 nm (c). The dots are the data, the line is the result of the fit, and residuals (data minus fit) shown above the spectra. The vertical axis for the residuals has the same scale as that for the spectra. The individual HF $F \rightarrow F'$ components are identified by letter according to the scheme shown in Fig. 2(a) for ${}^5S_2 \rightarrow {}^5P_1$, Fig. 2(b) for ${}^5S_2 \rightarrow {}^5P_2$, and Fig. 2(b) for ${}^5S_2 \rightarrow {}^5P_3$. Any unidentified peaks, and all the dips, are crossovers.

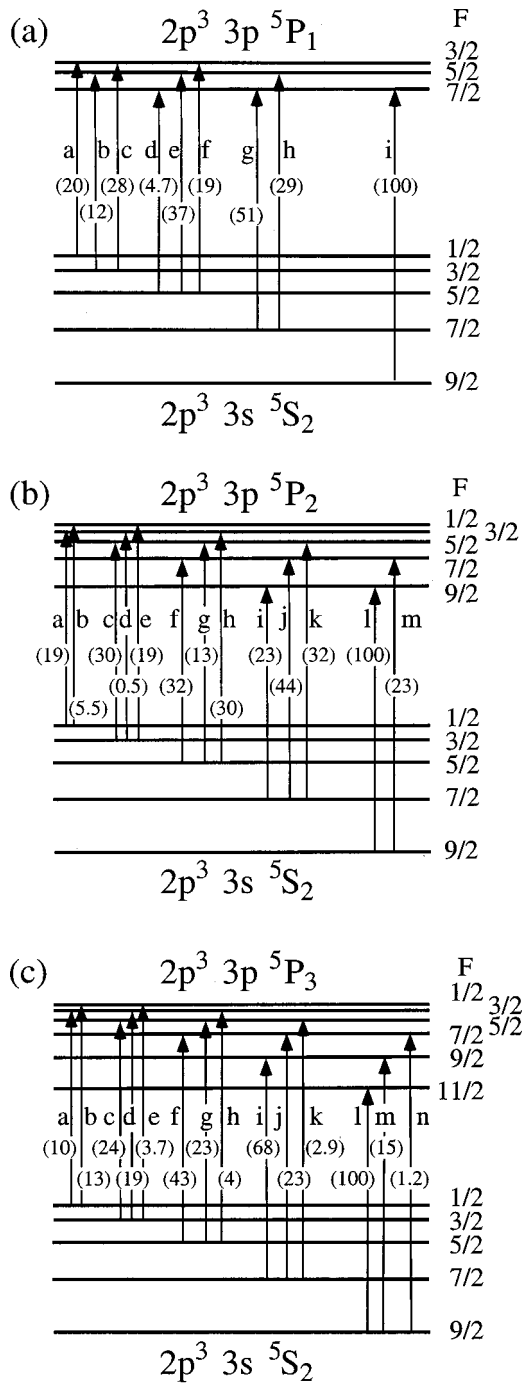


FIG. 2. Diagrams of the HFS of the upper and lower levels of ^{17}O in the three fine-structure transitions shown in Fig. 1. (a) identifies the HF transitions in $^5S_2 \rightarrow ^5P_1$, (b) identifies the HF transitions in $^5S_2 \rightarrow ^5P_2$, and (c) identifies the HF transitions in $^5S_2 \rightarrow ^5P_3$. Letters (a, b, c, etc.) represent the F values connected by a particular HF component: for instance, in (a), i represents the $F = 9/2 \rightarrow F' = 7/2$ component, which appears in the Doppler-free spectrum in Fig. 1(a) as the peak identified by the letter i . The numbers in brackets on the individual transitions are their calculated relative intensities within the multiplet.

150.127 MHz etalon fringes, and the linearized spectrum was then smoothed to give one data point every 2 MHz. The smoothed spectra were then fitted using initial estimates for

the HF coupling constants and isotope shifts. For the $^5S_2 \rightarrow ^5P_1$ transition, good values of the IS and A and B values for the upper and lower states in ^{17}O were available from Marin *et al.* (1993) [4]. However, no previous work has reported values for the A and B constants of the 5P_2 and 5P_3 states, or IS values for the $^5S_2 \rightarrow ^5P_2$ and $^5S_2 \rightarrow ^5P_3$ transitions. Instead, we identified the $F \rightarrow F'$ components of the $^5S_2 \rightarrow ^5P_2$ and $^5S_2 \rightarrow ^5P_3$ transitions using the previous values of $A(^5S_2)$ and the predicted relative intensities of the HF components. Initial values of the spectroscopic constants were then found using the positions of some of the features in each spectrum. The spectra were fitted assuming that the spectral features were Voigt profiles with different amplitudes but identical Lorentzian widths in each isotope. The Gaussian component of the line shape arises from the non-zero crossing angle of the pump and probe-laser beams, and the FWHM width of this component was fixed at 8 MHz, the value obtained from the measured crossing angle and the fitted width of Doppler-limited spectra of the transition for ^{16}O . The Lorentzian widths of ^{16}O , ^{17}O , and ^{18}O components were allowed to be different, though all the ^{17}O components (real transitions and crossovers) had their widths fixed to be equal. The positions of the ^{16}O and ^{18}O components are each determined by just one parameter (since neither isotope exhibits HFS). The positions of all the ^{17}O features in the fit were determined only by the center of gravity of the multiplet, and the magnetic dipole and electric quadrupole HF coupling parameters of the upper and lower states [9]. Most of the crossovers shared either an upper or a lower state, but some were identified that shared no common state, which probably arise as a consequence of collisional pumping. The fits also included a background offset and slope, and some of the more prominent features were given small Gaussian pedestals in the fit. Inclusion of the pedestals, whose centers were fixed to the centers of the narrow Voigt features, improved the chi-squared parameter for each fit by some 20%–30% from the fits that did not include the pedestals, but had negligible effect on the fitted HFS constants or centers of gravity of the multiplets. These Gaussian pedestals are caused by velocity-changing collisions in the discharge, and their relatively narrow width (approximately 200–300 MHz FWHM, compared with the full Doppler FWHM of 2.5 GHz) is a consequence of incomplete thermalization of the sample of atoms by collisions. That is, oxygen atoms undergo only a few collisions while they interact with the laser beam, and these collisions are “weak” in that the velocity change of an oxygen atom is small compared with the rms velocity of the oxygen atoms in the discharge [12].

Examples of fitted Doppler-free spectra of the $^5S_2 \rightarrow ^5P_J$ multiplet are shown in Fig. 1. Figure 1(a) shows the $^5S_2 \rightarrow ^5P_1$ transition at a vacuum wavelength of 777.753 nm, Fig. 1(b) the $^5S_2 \rightarrow ^5P_2$ transition at 777.630 nm, and Fig. 1(c) the $^5S_2 \rightarrow ^5P_3$ transition at 777.408 nm. The dots are the data, the line is the result of the fit, and residuals (difference between the data and the fit) are shown on a separate scale above the spectra. The spectra in Fig. 1 were taken at pressures between 30 and 50 mTorr, 90 W of microwave power, and $\sim 100 \mu\text{W}/\text{mm}^2$ laser intensity. Under these conditions, the linear absorption of the probe laser through the discharge

TABLE I. Magnetic dipole HFS coupling constants (A) and electric quadrupole HFS coupling constants (B) for the 5S_2 , 5P_1 , 5P_2 , and 5P_3 levels of ${}^{17}\text{O}$. The errors quoted for our experiment are one standard deviation of the mean.

Level	This experiment		Previous work	
	A (MHz)	B (MHz)	A (MHz)	B (MHz)
5S_2	-97.93 ± 0.10		-98.59 ± 0.43^a -96.7^b	
5P_1	-25.83 ± 0.10	0.0 ± 0.2	-26.39 ± 0.57^a	-0.3 ± 1.8^a
5P_2	-24.47 ± 0.11	0.9 ± 0.8		
5P_3	-18.70 ± 0.05	-0.2 ± 0.5		

^aReference [4].

^bReference [5].

was 20%–30%, and the Doppler-limited absorption FWHM was 2.5 GHz. In Fig. 2, we show the positions of the upper and lower HF states in ${}^{17}\text{O}$, the allowed HF transitions (identified by the letters: a, b, c, etc.), and their expected relative intensities, for the ${}^5S_2 \rightarrow {}^5P_1$ transition [Fig. 2(a)], the ${}^5S_2 \rightarrow {}^5P_2$ transition [Fig. 2(b)], and the ${}^5S_2 \rightarrow {}^5P_3$ transition [Fig. 2(c)]. In the spectrum shown in Fig. 1(a), the individual HF $F \rightarrow F'$ components are identified by the letter each is assigned in Fig. 2(a), and similarly the components in Fig. 1(b) are identified in Fig. 2(b), and the components in Fig. 1(c) are identified in Fig. 2(c). Unlabeled peaks, and all the dips in the Doppler-free spectra are crossover resonances (some of the real transitions are obscured by crossovers, and are not labeled in Fig. 1).

In all of our spectra, the ${}^{16}\text{O}$ peak goes off-scale vertically, but the signal-to-noise ratio was good enough to find the center using data from the wings. In each transition the hyperfine structure of ${}^{17}\text{O}$, combined with the effect of crossover resonances resulting from the use of saturated absorption spectroscopy, causes a complex spectral signature. For instance, in Fig. 1(b) there were 12 real HF transitions (the $F = 3/2 \rightarrow F' = 3/2$ component was too weak to manifest itself in our spectra) and 27 crossovers, all of which were identified in the spectrum, and fitted to find their amplitudes. Inclusion of all these effects (crossovers in ${}^{17}\text{O}$, different spectral widths for the different isotopes, and some Gaussian

pedestals) resulted in very good fits to the data, as can be seen from the scale of the residuals in Fig. 1.

The IS values and the magnetic dipole and electric quadrupole HF coupling constants we obtained for the 5S_2 and ${}^5P_{J'}$ states of ${}^{17}\text{O}$ are given in Tables I and II, respectively. In Tables I and II, all units are MHz, and the positive values for the isotope shifts indicates that the IS are normal for these transitions. The quoted errors are one standard deviation of the mean, and were obtained by adding in quadrature three different contributions. First, for each spectrum our fitting program found A values, B values, and center of gravity frequencies for each isotope, along with an estimate of the fitting uncertainty of a particular parameter obtained from that fit. These uncertainties were obtained from the square roots of the diagonal elements of the covariance matrix of the fit. Second, standard deviations were obtained by statistical analysis of many sets of IS, and A and B values, each set being obtained from the fit of one spectrum. Finally, our errors include an allowance for the uncertainty inherent in the linearization of each spectrum, which has two components. First, the measured value of the confocal etalon's free spectral range has an uncertainty that results in a small uncertainty in the frequency scale, and which amounts to no more than 0.28 MHz in the largest IS interval reported here. Second, and more significant, is the uncertainty associated with linearization of the laser scans using the 150.127 MHz

TABLE II. Experimental values of the isotope shifts (measured IS) of the ${}^5S_2 \rightarrow {}^5P_1$, ${}^5S_2 \rightarrow {}^5P_2$, and ${}^5S_2 \rightarrow {}^5P_3$ transitions. Also given are calculated values for the normal mass shift (NMS). The errors quoted for our experimental data are one standard deviation of the mean.

Transition	Shift	Measured IS (this paper) (MHz)	Measured IS (previous work) (MHz)	NMS (MHz)
${}^5S_2 \rightarrow {}^5P_1$	${}^{18}\text{O} - {}^{16}\text{O}$	1944.66 ± 0.79	1943.8 ± 0.5^a	1472.05
	${}^{18}\text{O} - {}^{17}\text{O}$	909.98 ± 0.73	911.3 ± 2.1^a	691.10
${}^5S_2 \rightarrow {}^5P_2$	${}^{18}\text{O} - {}^{16}\text{O}$	1944.49 ± 0.85		1472.28
	${}^{18}\text{O} - {}^{17}\text{O}$	909.94 ± 0.73		691.21
${}^5S_2 \rightarrow {}^5P_3$	${}^{18}\text{O} - {}^{16}\text{O}$	1945.03 ± 0.77		1472.70
	${}^{18}\text{O} - {}^{17}\text{O}$	910.33 ± 0.70		691.40

^aReferences [3] and [4].

markers from the confocal etalon. The scans are linearized by finding the channel numbers (in the oscilloscope raw data file) of the centers of gravity of the etalon transmission peaks, which we assume to be spaced exactly 150.127 MHz apart. The frequencies of the transmission peaks' centers of gravity are then fitted to a third-order polynomial function of their channel numbers, and the coefficients obtained from this fit then used to synthesize the frequency scale of the spectrum. The uncertainty introduced by adopting this method is estimated by finding the root-mean-square deviations of the etalon transmission peak centers of gravity from their assumed positions. This rms deviation was found to have an average value of 0.48 MHz, evaluated for a sample of 25 spectra. Hence, we had to assume that the frequency of any given peak in our spectra was uncertain by ± 0.48 MHz. For the IS values (intervals), this translates to an uncertainty of 0.68 MHz, which was added in quadrature with the errors from the sources above for the IS values reported in Table II. However, in adding this uncertainty into the errors for the A and B values, a different procedure was used. Since we fitted the entire ^{17}O spectrum to give the A and B values directly, and not from differences of peak positions, we treated the 0.68 MHz interval uncertainty as an additional linearization uncertainty of $(0.68 \text{ MHz}/\text{largest HFS splitting in } ^{17}\text{O}) \times (A \text{ or } B \text{ value})$ for the resultant uncertainties in the A and B values of ^{17}O . (The largest HFS splitting in ^{17}O was the frequency difference between the lowest HFS component and the highest, or some 1000 MHz.) This small uncertainty was added in quadrature with the errors from the sources above for the A and B values reported in Table I. As can be seen in Table I, the uncertainties of the B values are somewhat larger than the A value uncertainties. This is a manifestation of the fact that the position of a HF component in ^{17}O (relative to the center of gravity) is generally much more strongly dependent on the A values of the upper and lower states than the corresponding B values, due to the different sizes of the angular momentum factors that multiply the HFS coupling constants. When fitting different intervals in a spectrum that have certain measurement uncertainties to obtain the HFS constants, the resultant uncertainties in the B values will thus be larger than in the A values.

In all of the fits that contributed to the data shown in Tables I and II the electric quadrupole coupling constant of the 5S_2 state of ^{17}O was fixed to be zero. However, as noted above, polarization of the closed $1s$ and $2s$ orbitals by the three $2p$ electrons mixes the $2p$ subshell with other orbitals. Consequently, the $2p^3$ electrons do not couple exactly in 4S in oxygen and hence the electric quadrupole coupling constant of the 5S_2 state of ^{17}O should be nonzero. This effect also occurs in the $2p^3\ ^4S_{3/2}$ state of ^{14}N , where both A and B are expected to be zero, but have been measured to be 10.45 MHz and 1.27 Hz, respectively [13]. Hence we also tried fitting our ^{17}O spectra with a floating value for $B(^5S_2)$, but the results of these fits were inconclusive. While the average of all the fits seemed to reveal a nonzero value for $B(^5S_2)$, of order 1–2 MHz, the value obtained was systematically different for the $^5S_2 \rightarrow ^5P_1$, $^5S_2 \rightarrow ^5P_2$, and $^5S_2 \rightarrow ^5P_3$ transitions. In addition, there seemed to be a strong correlation between the B values of the 5S_2 state and the 5P_J state

obtained from a single fit. We attributed this correlation to the fact that the positions of many features in the ^{17}O spectrum are sensitive to the difference of the B values of the lower and upper states, rather than to the individual lower and upper state B values. We therefore concluded that the value of $B(^5S_2)$ was too small to be recovered successfully from our data. We note that fixing $B(^5S_2)=0$ gave very consistent values for $A(^5S_2)$ (within 0.04 MHz) from the three transitions.

As can be seen, the data in Tables I and II are reasonably consistent with previous experimental results for the IS and HFS coupling constants. Our set of values for the HFS coupling constants in Table I are significantly more precise than the previously reported values, and much more complete. The set of IS values given in Table II have about the same precision as previous values, but is also more complete. The $^{18}\text{O}-^{16}\text{O}$ and $^{18}\text{O}-^{17}\text{O}$ IS of the $^5S_2 \rightarrow ^5P_1$ transition agree within the errors with the results of Marin *et al.* (1992) [3], which were made using heterodyne techniques. Our values for the magnetic dipole and electric quadrupole coupling constants of the 5P_1 state agree with the results of Marin *et al.* (1993) within one standard deviation of that paper's experimental results [4]. However, our value for $A(^5S_2)$ is different from the result of Ref. [4] by more than one standard deviation of the previous paper's results, though the values agree within two standard deviations. We believe that the origin of this discrepancy is in the lower resolution of the previous results. For instance, ours is the first work on the Doppler-free spectra of this multiplet to reveal the inverted crossovers apparent in Figs. 1(a) through 1(c). Such crossovers were not allowed for in the fitting routine reported in Ref. [4], though they appear to be present in the spectra shown in Fig. 3 of that paper. Finally, we note that our value for $A(^5S_2)$ is in better agreement with the theoretical value for this parameter calculated by Godefroid *et al.* [5], though there is still a significant difference between our experimental value and the theoretical result.

The fitted values for the relative intensities of the ^{17}O HF components were all generally in agreement with the theoretical values shown in Fig. 2 within $\pm 20\%$, with the exception of real HF components that were partially or totally obscured by crossovers. In fitting our spectra, we allowed the linewidths for the different isotopes to have different widths so that the effect of the strong (and off-scale) ^{16}O line did not dominate the fitted widths of the other two isotopes' transitions. As a consequence of this, we found that in all our spectra, the Lorentzian FWHM widths of the different isotopes were slightly different, being narrower by some 2–3 MHz for ^{18}O than for ^{16}O or ^{17}O , which usually had widths similar to within 1 MHz. The minimum FWHM of the saturated absorption signals was 15 MHz for the ^{16}O signal and ^{17}O HF components, but the ^{18}O signal had a minimum FWHM of 12 MHz. Obviously, the natural linewidths of these transitions should be isotope independent, as should any collisional broadening effects since the dominant collision partners for all O atoms in our discharge are O_2 molecules. The only mechanism that could explain different linewidths for the different isotopes is if the pump-laser intensity was significantly different for ^{18}O than ^{16}O and ^{17}O due to

linear absorption in the discharge. Since our pump-laser intensity was several times the saturation intensity of the transitions (see below), different pump-laser intensities will result in different linewidths in the saturated absorption spectra. However, it is unclear why this should lead to a narrower linewidth for ^{18}O than for the other two isotopes, and not a larger linewidth, given the relative isotopic abundances.

The minimum observed Lorentzian widths are a factor of 3 larger than the 4 MHz value expected on the basis of the measured lifetimes of the 5S_2 and $^5P_{J'}$ states [6,7]. The minimum widths were observed at a pressure of 80 mTorr at a pump-laser intensity of $\sim 100 \mu\text{W}/\text{mm}^2$, the minimum intensity used in these experiments. Between 0.3 Torr and 0.03 Torr, the pressure broadening coefficient was of order 10 MHz/Torr, so the excess widths cannot be attributed to collisional broadening on the basis of our experimental evidence. We were unable to fully investigate the effect of the microwave power to the discharge, as the discharge became unstable at powers below 60 W, but we found no significant broadening attributable to the discharge power in the range 70–100 W. It is probable that the excess widths are due to laser power broadening. We calculated the saturation intensities of the $^5S_2 \rightarrow ^5P_{J'}$ transitions in the limit of negligible collisional quenching to be in the range $(1-4) \times 10^{-2} \mu\text{W}/\text{mm}^2$. The most significant factor determining these values is the low-radiative decay rate of the 5S_2 state of $5.56 \times 10^3 \text{ s}^{-1}$. However, the true relaxation rates of the

5S_2 and $^5P_{J'}$ states in the discharge will be larger than the radiative decay rates due to collisional quenching. Based on measured values for quenching coefficients of the 5S_2 and $^5P_{J'}$ states due to collisions with O_2 molecules [14,15], we estimate the saturation intensities to be in the range 25–90 $\mu\text{W}/\text{mm}^2$ at 100 mTorr, which indicates it is probable that we were intensity broadening our spectra even at the lowest intensity used in these experiments. Finally, it should be noted that collisional quenching of the 5S_2 state reduces the lifetime of this state in the discharge from 180 to $\sim 1 \mu\text{s}$ [14]. Hence, we were unable to make measurements by chopping the microwaves and only taking data points with the discharge off since the 5S_2 states decay too quickly.

We have measured IS between the three stable isotopes of atomic oxygen in the three transitions of the $^5S_2 \rightarrow ^5P_J$ multiplet near 778 nm using Doppler-free saturated absorption spectroscopy with an external cavity diode laser. In addition, we have measured the magnetic dipole and electric quadrupole HF coupling constants of the 5S_2 , 5P_1 , 5P_2 , and 5P_3 states of ^{17}O . Our set of measurements is more extensive and generally more precise than previously published results, and we hope that these data will stimulate more theoretical study of these states.

Funding for these experiments has been provided by Colby College under the Natural Sciences Grant Program, by the Research Corporation, and by the NSF (Grant No. PHY-9601638).

-
- [1] G. M. Tino, L. Hollberg, A. Sasso, M. Inguscio, and M. Bar-santi, *Phys. Rev. Lett.* **64**, 2999 (1990).
 - [2] M. de Angelis, M. Inguscio, L. Julien, F. Marin, A. Sasso, and G. M. Tino, *Phys. Rev. A* **44**, 5811 (1991).
 - [3] F. Marin, P. De Natale, M. Prevedelli, M. Inguscio, L. R. Zink, and G. M. Tino, *Opt. Lett.* **17**, 148 (1992).
 - [4] F. Marin, C. Fort, M. Prevedelli, M. Inguscio, G. M. Tino, and J. Bauche, *Z. Phys. D: At., Mol. Clusters* **25**, 191 (1993).
 - [5] M. R. Godefroid, G. Van Meulebeke, P. Jönsson, and C. Froese Fischer, *Z. Phys. D: At., Mol. Clusters* **42**, 193 (1997).
 - [6] N. J. Mason, *Meas. Sci. Technol.* **1**, 596 (1990).
 - [7] J. Bromander, N. Durić, P. Erman, and M. Larsson, *Phys. Scr.* **17**, 119 (1978).
 - [8] D. A. Tate and D. N. Aturaliye, *Phys. Rev. A* **56**, 1844 (1997).
 - [9] D. A. Tate and J. P. Walton, *Phys. Rev. A* **59**, 1170 (1999).
 - [10] K. B. MacAdam, A. Steinbach, and C. Wieman, *Am. J. Phys.* **60**, 1098 (1992).
 - [11] F. C. Fehsenfeld, K. M. Evenson, and H. P. Broida, *Rev. Sci. Instrum.* **36**, 294 (1965).
 - [12] C. Brechignac, R. Vetter, and P. R. Berman, *Phys. Rev. A* **17**, 1609 (1978).
 - [13] J. M. Hirsch, G. H. Zimmerman III, D. J. Larson, and N. F. Ramsey, *Phys. Rev. A* **16**, 484 (1977).
 - [14] L. Julien, J. P. Descoubes, and F. Laloë, *J. Phys. B* **12**, L769 (1979).
 - [15] P. J. Dagdigian, B. E. Forch, and A. W. Miziolek, *Chem. Phys. Lett.* **148**, 299 (1988).